Optica Applicata, Vol. XVII, No. 3, 1987

Diffraction model of the laser channel with stationary approximation

ADAM DUBIK, ANTONI SARZYŃSKI

Kaliski Institute of Plasma Physics and Laser Microfusion, P.O. Box 49, 00–908 Warszawa, Poland.

In this paper the equations describing a simplified diffraction model of the laser channel with spatial filter has been described. The corresponding equations have been solved by using the method of finite differences. The accuracy of the obtained numerical solutions has been discussed. Some examples of optimization of laser channel configuration at the assumed criteria for the system perfection are given. Apodization, relaying, and filtration have been taken into account. The possible effects following from the thermooptical focusing (or defocusing) of the light beam resulting from the rod heating during pumping were considered.

1. Introduction

Optimization of the high power laser systems, used in investigations of the controlled thermonuclear fusion, X-ray lasers, high pressure obtaining, X-ray lithography and so on, requires the application of numerical methods [1], since they allow us to introduce the suitable corrections to the design of the laser systems before their building, to determine the places of particular danger as well as to simulate the critical working conditions of the laser system without damaging the real system.

In the course of the last years a considerable progress has been achieved in the design of codes used to numerical modelling and optimization of the laser systems. Nowadays, some of those codes are used to model the operation of the modern laser systems in the way assuring a very high agreement between the calculations and experiment [1].

In the present paper, the construction of the code of similar kind meeting the needs of the Institute of Plasma Physics and Laser Microfusion has been described. The examinations were restricted to the diffraction effect occurring in the apertures places within the laser system (the housings of the amplifying heads, the pinholes) to the apodization, relaying, filtration and thermooptical phenomena.

The equations were solved by employing the method of finite differences. The axial-symmetric approximation has been applied, assuming the process stationarity.

In Section 2 of the present work, the equations of the problem under considerations are derived, in Sect. 3 the accuracy of the method is described, in Sect. 4 the results of the calculations are given, and Sect. 5 includes a recapitulation.

The work presented allowed us to verify the calculations concerning the laser channel based on the geometrical optics method, as well as to determine the forseen

field distribution in different places of the system. It also enabled a better understanding of the causality of the effects occurring in the high power lasers. The complete exploitation of the results of calculations in the high power lasers will be possible after developing the code to the form rendering possibility of modelling the amplification and the self-focusing of the radiation propagating in a nonstationary way. The works in this direction are being carried out and will be the subject of the next publication.

2. Equations and the solving method

Such phenomena as the propagation of radiation, amplification, filtration and self-focusing in the laser system may be described with the help of the so-called parabolic equation [1]–[5]

$$\frac{1}{c}\frac{\partial E}{\partial t}+2ik\frac{\partial E}{\partial z}+\frac{1}{r}\frac{\partial}{\partial r}\left(r\frac{\partial E}{\partial r}\right)=2ikEF(r, z, t) \tag{1}$$

where: E – complex amplitude of the electric field of the wave,
$k = 2\pi/\lambda$ – wavenumber,
z – coordinate along the laser axis determining the dominating direction of the radiation propagation,
r – radius in the cross-section of the beam,

$$F(r, z, t)=\frac{g-\alpha}{2}+ik\left[\frac{\delta n(r, z)}{n_0}+2\frac{f(r)}{L}+n_2\frac{|E|^2}{2n_0}\right] \tag{2}$$

is the function describing the influence of the material media on the radiation propagation (where: g – coefficient of amplification, α – linear losses, n_0 – linear index of refraction, $\delta n(r, z)$ – function describing the volume nonuniformity of the refractive index, $f(r)$ – function describing the shape of the front surfaces of the rods, $n_2|E|^2$ – change of the refractive index connected with the nonlinear interaction between the radiation and the medium (self-focusing)).

The reduced aims of this work allow us to simplify Eq. (1) to a high extent. By applying the stationary approximation and neglecting amplification, losses, self-focusing, and deformation of the front surfaces of the rods as well as restricting the investigation to diffraction, relaying, filtration, and volume thermooptical effects it was possible to write Eq. (1) in the form

$$2ik\frac{\partial E}{\partial z}+\frac{1}{r}\frac{\partial}{\partial r}\left(r\frac{\partial E}{\partial r}\right)=-2k^2E\frac{\delta n(r, z)}{n_0}. \tag{3}$$

The solution of Eq. (3) exists under the following boundary and initial conditions:

$$\lim_{r\to 0}\frac{\partial E}{\partial r}=0, \qquad \lim_{r\to\infty}E(r, z)=0 \tag{4}$$

$$E(r, z=0)=E_0(r). \tag{5a}$$

In our calculations it has been most frequently assumed that

$$E_0(r) = \exp[-3.455(r/a)^{N_d}] \tag{5b}$$

which is the super-Gaussian function with $N_d = 2$–200 (apodization exponent).

Equation (3) may be solved in the general case by using numerical methods, while the analytic solutions are possible only in particular and simple cases. One of the numerical methods making it possible to solve the Eq. (3) is the difference method [2]–[5]. This method has been applied also in this work. It should be noticed that for numerical solution of Eq. (3) the Talanov transformation prove to be very useful [5], [6].

3. Accuracy of the method

In paper [5] the accuracy of the difference method has been determined for a simple system of aperture-lens type. In the laser systems containing the spatial filters (relay systems) the radiation suffers from multiple retransmission and propagates usually to great distances. In this case, the errors of the applied method of finite differences cumulate during the calculations which may lead to significant perturbations of the sought solution. Hence, a discussion of the error of this method wider than that given in [5], [6] seems to be necessary.

The magnitude of $R_{\max}$ equal to the ratio of the numerical lattice radius to the beam radius has a strong influence on the accuracy of the numerical solution. In the present paper, the beam radius (denoted by the letter a) in the near field is identified with the radius of the field forming aperture. In the case of super-Gaussian beam (5b) a denotes the radius for which the field is 10^{-3} times less than that on the axis ($r = 0$). During the propagation in the laser system the beam may be magnified (demagnified). Then, in accordance with principles of the geometric optics the value of a was changed suitably. On the other hand, in the far field (in the vicinity of the beam foci) a was understood as

$$a' = \lambda f/a_s \tag{6}$$

where: λ – wavelength of the radiation,
f – focal length of the lens focusing the beam,
a_s – radius of the beam in the lens plane ($r_0 = 0.61\ \lambda f/a_s$ – determines the radius of the zero order of the rectangular distribution in the far field).

The accuracy of the solution depends also on the following step values: Δr – spatial step, and Δz – that along the direction of the beam propagation

$$\begin{aligned} &\text{in the near field: } \Delta r = a/N, \\ &\text{in the far field: } \Delta r' = a'/N_0. \end{aligned} \tag{7}$$

In most cases N, N_0 and $R_{\max}$ were assumed to be equal to 250, 50 and 3, respectively. The step Δz was chosen in accordance with the formula

$$\Delta z = 8\pi \Delta r^2/\lambda. \tag{8}$$

The calculations have shown that for this value of the step Δz the step Δr (resp. $\Delta r'$) and R_{max} are decisive as far as the solution accuracy is concerned.

In the case of the Gaussian beam $E(r, 0) = \exp(-Br^2)$ it is easy to obtain a numerical solution of high accuracy. This follows from the fact that the rate of changes of this function is relatively slow (for $B = 1$–2). In Figure 1 the graphs of the

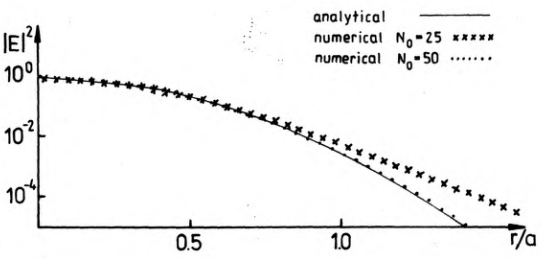

Fig. 1. Comparison of the analytic and numerical solutions for the Gaussian beam

radiation power density at the focus are presented for both the Gaussian beam obtained from the analytic formula and that received by numerical solution. This figure illustrates the influence of the mentioned value of N_0 on the solution accuracy. A very good consistence of the numerical solution with that obtained in analytical way is observed when increasing the value of N_0 from 25 to 50. In this case, the laser system consisted of an amplitude screen forming the $\exp(-Br^2)$ field and a lens. Also, for the more complex systems (for instance, with four relay systems) a very good agreement between the analytical solution and that of the numerical type was achieved. For the Gaussian beam the field values in each plane of the relay system may be easily calculated from the analytical formula. However, in the case of super-Gaussian beam ($N_d > 2$) the exact solution is known only in the image planes of the realy systems, i.e., the field distribution in those planes should be the same as that in the initial plane [7]. If the magnification of the retransmitter is different from unity, the solution should be scaled in accordance with the Talanov transformation. This fact has been exploited to examine the accuracy of the numerical solution for the super-Gaussian beams. The above assumption loses its validity if any diaphragms or pinholes appear in the system.

In Figure 2 the graphs of radiation power density in the image plane are shown for the beam of initial distribution

$$E_0(r) = \exp[-3.455(r/a)^{10}]. \tag{9}$$

It has been assumed for the calculation that $N = 250$, $N_0 = 50$, and $R_{max} = 3$ and 5. The strong influence of the parasitic reflections from the grating edge on the numerical solution is visible. For a sufficient distance of the grating edge from the beam axis (in this case $R_{max} = 5$) the error falls down below 1%. This strong influence of the grating edge in the considered case of single relaying may be explained by the fact that the beam incident on the lens was of distribution characterized by a small Fresnel number ($F \sim 1$). Therefore, at the distances from the axis equal to several beam radii the values of the field are comparable with those at

the axis vicinity. Thus, the ratio of the grating radius to that of the beam decreases. For the same initial field distribution (9) and the system containing three relay systems the difference between the initial distribution and the one recovered in the image plane of the third relay system does not exceed 4% (Fig. 2). In this case

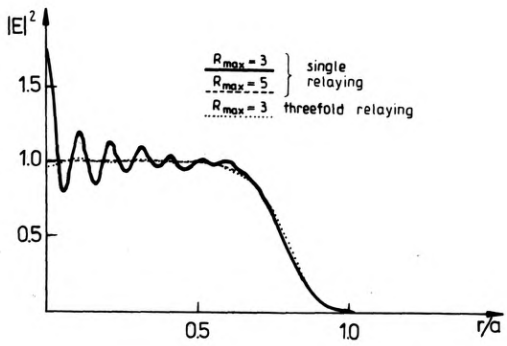

Fig. 2. Influence of the lattice edge position R_{max} on the imaging accuracy of the distribution $\exp[-3.455(r/a)^{10}]$ in the relay system image plane

(threefold relaying) the focal lengths of the relay system lenses and their positions were chosen in such a way that the Fresnel numbers in the space between the filters satisfy the following condition:

$$|F| \gg 1. \tag{10}$$

Therefore, the ratio of the grating radius to that of the beam both in the near field and in the far field, respectively, took the sufficiently high values which reduced the influence of the parasitic reflections on the solution.

By using this method it is much more difficult to obtain an accurate imaging of the super-Gaussian beam, for instance of $\exp[-3.455(r/a)^{100}]$ kind. Firstly, a low energy "tail" appears at a distance $r = 3$ from the axis. In this case, high values for R_{max} must be assumed in order to avoid the influence of the parasitic reflections. Secondly, the spatial scale of the diffraction peaks for this beam is relatively small (high spatial frequency), therefore a small step of Δr should be used. Thirdly, in the far field the amplitude of the electric field strength of the Fourier spectrum of the beam decays slowly with the radius r (like $r^{-3/2}$), consequently, such data must be assumed:

$$\frac{r_{grat}}{a'} = \frac{NR_{max}}{N_0} \gg 10. \tag{11}$$

The fulfillment of these conditions restricts the speed of the available computer work as well as the capacity of their operational memory.

The restriction of parasitic reflections from the grating may be achieved by a suitable change of the boundary condition. To this end the condition

$$\lim_{r\to\infty} E(r, z) = 0, \tag{12}$$

the fulfillment of which is impossible in the case of a finite grating is replaced by the

assumption that the radiation is absorbed at the edge. The practical realization of this assumption is fulfilled in such a way that after determining the field at the sequent plane $z^{n+1} = z^n + \Delta z$, the field is zeroed at five nodal points adjacent to the lattice edges.

In Figure 3 the results of this operation obtained under the condition

$$R(R_{max}, z) = 0 \tag{13}$$

are denoted by a thin line (the edge of the lattice reflects the radiation), the solution for the "absorbing" edge being denoted by the thick line. These solutions have been obtained after fourfold relaying for the other unchanged data.

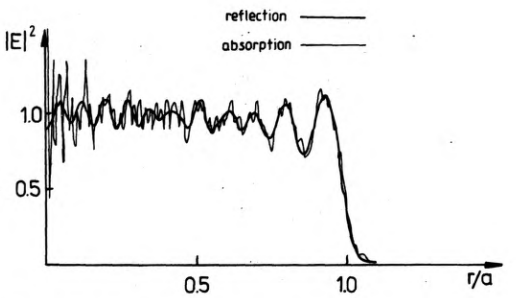

Fig. 3. Influence of the way of approximation of the boundary condition $\lim_{r\to\infty} E(r, z) = 0$ on the finite lattice on the imaging accuracy of the distribution $\exp[-3.455(r/a)^{100}]$ in the image plane after a fourfold retransmission, thin line – the edge reflects the radiation, thick line – the edge absorbs

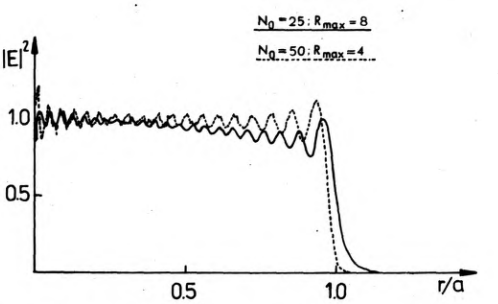

Fig. 4. Total influence of the lattice edge position R_{max} and the step $\Delta r' = a'/N_0$ on the imaging accuracy of the distribution $\exp[-3.455(r/a)^{100}]$ in the image plane after fourfold relaying

As it follows from Fig. 3, the parasitic solutions emerging at the lattice edge and leading to small scale modulation in the beam cross-section distribution could be "filtered" out of the solution, owing to the edge "absorption".

The increment in the numerical lattice dimensions decreases the amplitude of oscillations, increasing their frequency. In Figure 4 the solutions has been plotted for:

$R_{max} = 8$, $N_0 = 25$ – continuous line,

$R_{max} = 4$, $N_0 = 50$ – broken line.

The application of the difference method to the rectangular distribution (infinite exponent of apodization) resulted in a solution suffering from a high error (about 50%).

The oscillations of the numerical solution around the exact one are due to the Gibbs effect. Each method taking account of the finite Fourier spectrum (for instance, the Hankel transform method [8]) or finite number of the eigenfunction (for instance, the method of Hermite–Gauss functions [9]), and applied to the approximation of the rectangular distribution approximates this distribution with

the error of 5–10% (comp. also [10]). This has been exemplified in Fig. 5 by showing the result of approximation of the rectangular distribution with the help of finite sum of Laguerre–Gauss functions (which are eigenfunctions of the stationary parabolic equation of cylindric symmetry).

In the conclusions it should be stated that in the case of super-Gaussian distribution and not too high apodization the difference method allows us to obtain

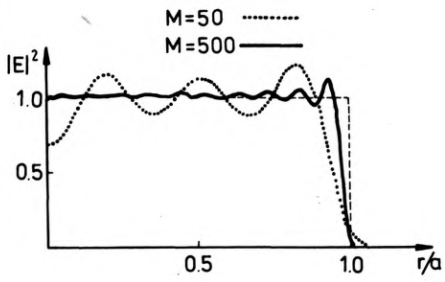

Fig. 5. Influence of the number of terms M of the finite sum of the Laguerre–Gauss functions on the approximation accuracy of the rectangular distribution

the solution suffering from small errors. However, this method requires some caution when interpreting the results, since in some cases it is difficult to distinguish the numerical effects from the physical ones. The difference scheme has its own modulation frequency of the solution depending on the step Δr, the lattice size R_{max} and the Fourier spectrum range on the lattice NR_{max}/N_0 (comp. Figs. 3 and 4). In each variant of calculations the accuracy of results should be determined by changing not only the mentioned magnitudes Δr, R_{max} and N_0, but also the relations between them. This is the only way to distinguish the numerical effects from the physical ones.

In the further calculations it has been assumed that $R_{max} = 3$, $N = 250$, and $N_0 = 50$, which was conditioned by the operational memory and the speed of the used computer.

The difference scheme applied in this work approximates the parabolic equation with the error of $\Delta r^2/(6r)$ order. This accuracy proved to be sufficient. More accurate schemes ($\Delta r^2/36$ or $\Delta r^4/(12r)$) turn out to be more time-consuming (the time of calculation was 2–3 times greater), while they had the same eigenfrequencies following from the value N, N_0 and R_{max}. Thus, the reflections from the lattice edge (final lattice approximating the solution in the infinite space), the final Fourier spectrum of the beam and the final spatial step Δr were the main sources of errors. The kind of the difference scheme and the respective step Δz (less than that following from the formula (8)) had only minor influence on the solution error.

4. Examples of the laser system optimization

The laser model assumed in calculations was based on the assumption that only diffraction effects appear in the channel. Since the power distribution of the beam is modified by each aperture stopping a part of the radiation energy, the superposition

of the operation of many apertures occurring in the system may lead to local increases of the power occurring in the cross-section and exceeding many times the average power.

Due to simplification of the laser model following from assumption that only diffraction effects appear, the term of "optimal laser system"should be explained. In order to define the system quality, the following magnitudes attributed to the planes of amplifying heads have been assumed:

F – Fresnel number characterizing the power density distribution in the beam cross-section,

ϱ_c – diaphragming height (the value of the power density on the aperture edge of rod, for instance, referred to the value of radiation power density on the axis determined with the geometric optics approximation),

W_w – fill factor,

$$W_w = \int_0^{r_p} r|E|^2 dr \Big/ \left(\int_0^{r_p} r|E_g|^2 dr \right) \tag{14}$$

where $|E_g|^2$ – the value of the radiation power density on the axis of the beam determined again with the geometric optics approximation. The fill factor defined in this way may be related with the help of a respective coefficient to the damage threshold of the optical elements or to the effectiveness of energy extraction from the amplifying medium. The configurations of the laser channel assumed in calculation were chosen so that the energy losses in the apertures reaching usually the values of order of 0.1% (rarely 1%) might be neglected.

Therefore, the optimal laser system is here understood as a system for which the above defined parameters take the values from the following ranges:

$$|F| \gg 1, \quad 5 \times 10^{-4} < \varrho_c < 2 \times 10^{-3}, \quad 0.5 < W_w < 0.8. \tag{15}$$

In should be noticed that the high value of Fresnel number in the amplifier head position indicates that this head has been located at the vicinity of the image plane of the realy system. This assures a relatively uniform field distribution across the beam incident on the amplifier [7]. In the case ϱ_c, however, the small value of this parameter minimizes the influence of the apertures initiating the diffraction modulation of the distributions across the beam [3].

Now, the numerical results of the laser system modelling will be discussed.

Consider first the system without any relay systems, the scheme of which is shown in Fig. 6. In this system a beam of initial amplitude distribution in the cross-section of spherical phase and divergence $\alpha = 1.5$ mrad is subject to diffraction. This beam loses a part of energy (we take no account of amplification) due to diaphragming by the rod housings. The superposition of the initial diffraction distribution and the scatterings initiated by the successive apertures (rod housings) lead to a strong modulation of the power density distribution in the beam (Fig. 7). In the table under the Fig. 6 the values of parameters W_w, ϱ_c, F and P/P_0 – the relative loss of the power due to the stopping of a part of energy by the rod housing – have been also shown.

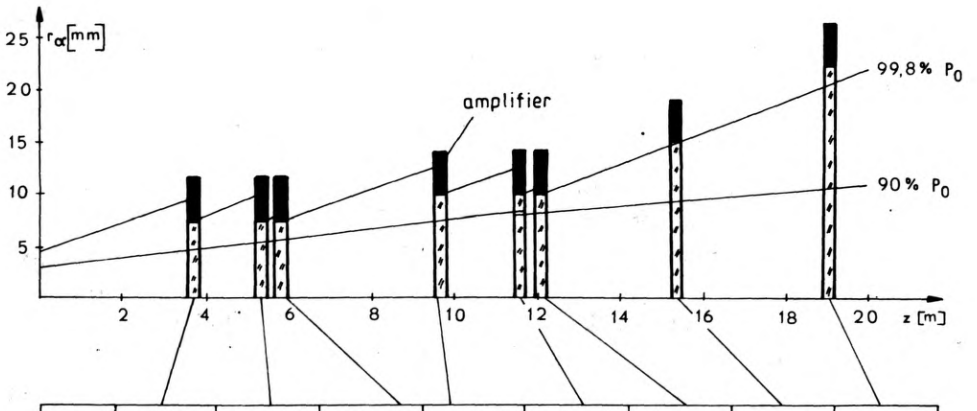

W_w	0.34	0.45	0.49	0.46	0.56	0.59	0.36	0.22
ϱ_c	1.5×10^{-3}	1.6×10^{-2}	2.2×10^{-2}	1.5×10^{-2}	7.2×10^{-2}	8.7×10^{-2}	2×10^{-5}	10^{-10}
$\Delta P/P_0$	7.9×10^{-4}	8.1×10^{-3}	2.4×10^{-3}	4.7×10^{-3}	1.76×10^{-2}	6.7×10^{-3}	4×10^{-6}	2×10^{-8}
F	5.6	4.4	4.1	3.2	3.0	2.9	2.7	2.5

Fig. 6. Scheme of the laser system without relay systems. The lines denoted by symbols 90% P_0 and 99.8% P_0 restrict the regions containing 90% and 99.8% of the beam power, respectively

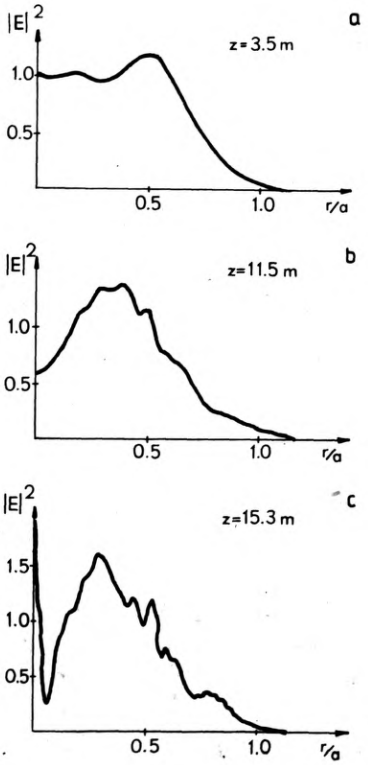

Fig. 7. Power density distribution in the beam incident on the front of the rods: **a** – I, **b** – V, **c** – VIII in the laser system without relay systems

Such a configuration is far from being optimal. The fill factor takes usually low values. The diaphragming height may be even as low as 8.7×10^{-2} which evokes a strong diffraction modulation of the field distribution on the sequent heads (Fig. 7). The local power density increases occurring in the amplified beam are disadvantageous for several reasons.

Firstly, the top power should not exceed the threshold power in order to avoid any damage of the optical elements. Therefore, in the system working with the nonuniform beam the average power should be reduced to such degree that the top power be lower than the threshold one. This causes, in turn, an incomplete exploitation of the power accumulation in the laser amplifier [1].

Secondly, for the power densities of GW/cm^2 order self-focusing plays an essential role. Consequently, the amplitude of the spatial uniformity modulation increases together with both the probability of optical element damage and the decay of energy extraction efficiency from the laser amplifiers. It happens that the insertion of relay systems to the system considered (scheme in Fig. 8) improves the laser quality. The fill factors in the planes of particular heads increase with the decreasing amplitudes of nonuniformities (Fig. 9). In the table under Fig. 8 we may notice that,

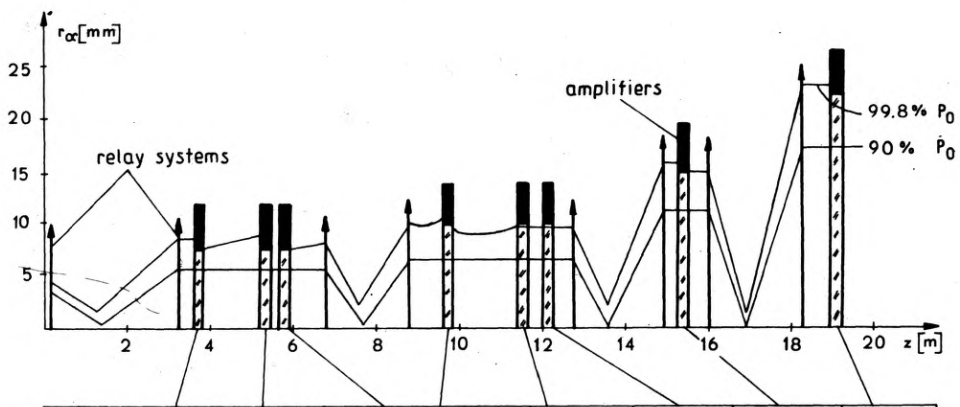

W_w	0.56	0.56	0.56	0.49	0.49	0.49	0.58	0.61
ϱ_c	1.3×10^{-2}	1.4×10^{-3}	3.0×10^{-4}	2.5×10^{-6}	9.1×10^{-5}	1.2×10^{-5}	8.2×10^{-4}	8.1×10^{-4}
$\Delta P/P_0$	2.6×10^{-3}	3.0×10^{-4}	3.7×10^{-5}	1.8×10^{-5}	1.7×10^{-5}	1.2×10^{-5}	9.3×10^{-5}	8.8×10^{-5}
F	-11.1	-17.9	-21.9	-21.9	-49.0	-77.4	-52.7	-47.8

Fig. 8. Scheme of the system with relay systems before optimization. The lines denoted by symbols 90% P_0 and 99.8% P_0 restrict the regions containing 90% and 99.8% of the beam power, respectively

on the average, the values of the fill factor increased substantially and that the heights of diaphragming ϱ_c decreased, while the absolute values of Fresnel number in the planes were high and had negative sign. This system, however, satisfies no more the criteria of optimal system defined above.

Firstly, in the plane I of the rod the diaphragming height ϱ_c is too great while the

Fresnel number – too small. Secondly, in the series of heads ⌀ 20 (IV, V and VI rod) the beam is of too small diaphragm which results in too low value of ϱ_c and consequently of W_w. The values given in table under Fig. 8 concern the beam of initial distribution $\exp[-3.455(r/a)^{10}]$. The increment of the apodization exponent up to 100 (Fig. 10) illustrates in a distinct way the shortcomings of this system. In this

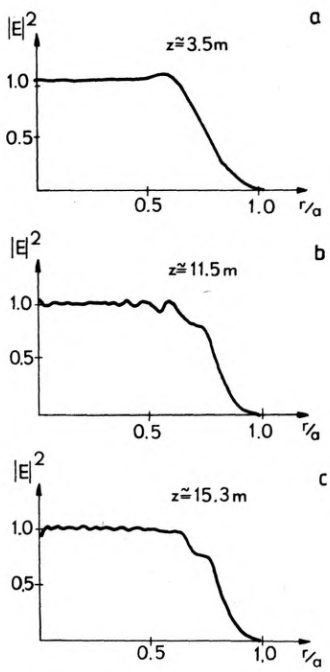

Fig. 9. Power density distribution in the beam incident on the front of the rods: **a** – I, **b** – V, **c** – VIII in nonoptimized laser system with relay system and the initial distribution of radiation $\exp[-3.455(r/a)^{10}]$

case a highly nonuniform distribution appears in the plane I of the head (see Fig. 10) and the high value of the fulfillment coefficient casuses an increment of ϱ_c (maximal value of $\varrho_c = 0.12$) increasing in this way the amplitude of spatial field modulation. From the comparison of Figs. 9 and 10 it follows that the laser system must be optimized for a definite initial distribution, since the optimized system for the beam ($E(r, 0) = \exp[-3.455(r/a)^{10}]$ for instance) will not be an optimum for the apodization exponent equal to $N_d = 100$.

It is the scheme of the laser system shown in Fig. 11 which satisfies the assumed optimizing criteria for $N_d = 10$. The focal lengths of the relay system lenses and the relative positions of the heads and the relay systems have been selected so as to fulfil the assumed criteria to the maximal degree. The methods of geometrical optics and the method of numerical analysis presented above were used to optimize the system. As it follows from Fig. 11 an additional divergence of the beam amounting to about 0.5 mrad in the channel with the heads of ⌀ 15 (rods I, II, III) and ⌀ 20 (rods IV, V, VI) turned out to be advantageous. The laser configuration shown in Fig. 11 is

optimal for $N_d = 10$ which corresponds to the working conditions of high power lasers used in our Institute.

The elaborated numerical code enables us also to examine the influence of the spatial filtration on the power density distribution in the planes of particular heads.

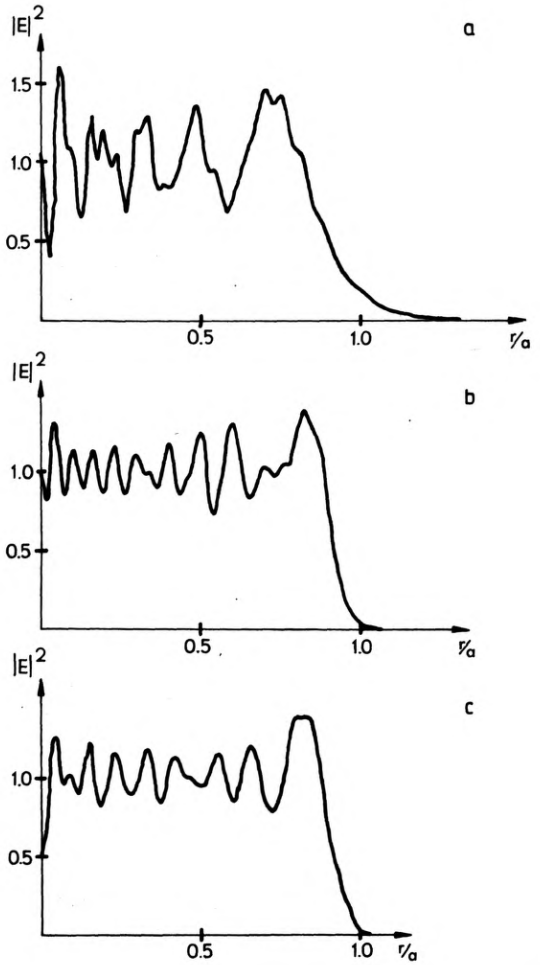

Fig. 10. The same as in Fig. 9, but for the initial distribution $\exp[-3.455(r/a)^{100}]$

In Figure 12 the graphs of power density are shown in the planes I, V and VIII of the rod for the system configuration (Fig. 11) and the apodization $N_d = 10$. In this case the fact that the beam filtration has been taken into account is visualized in Fig. 12**d** and 12**e**, in which power density distributions in the focusing planes of the sequent (I and II) spatial filters close before the pinhole planes are exemplified. It has been stated that for $N_d = 10$ the filtration changed only slightly the spatial distributions of the field in the planes of the amplifying heads.

In Figure 13 the configuration of laser system (intermediate between the nonoptimal (Fig. 8) and quasi-optimal (Fig. 11)) has been shown. The beam of field

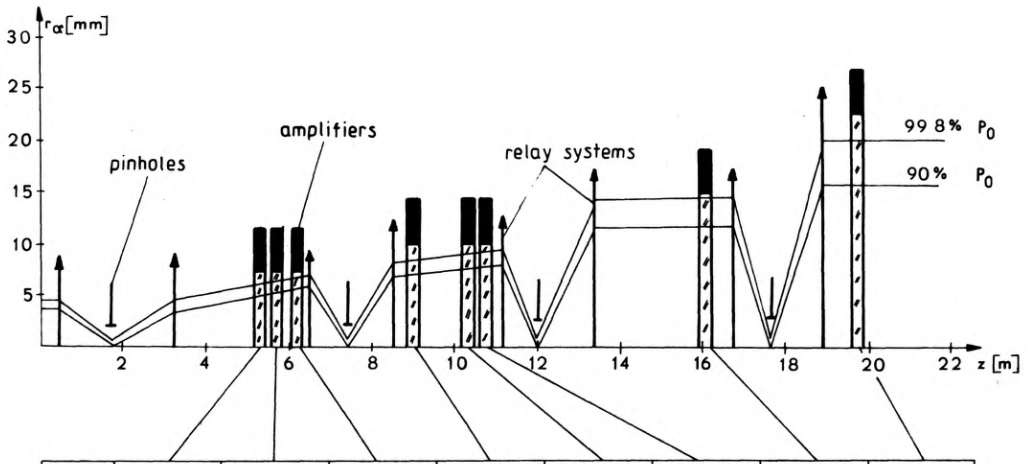

W_w	0.54	0.57	0.61	0.51	0.58	0.61	0.62	0.62
ρ_c	1.5×10^{-3}	9.4×10^{-5}	1.3×10^{-3}	4.0×10^{-4}	2.3×10^{-4}	8.6×10^{-4}	3.5×10^{-3}	2.9×10^{-3}
$\Delta P/P_0$	8.5×10^{-4}	6.5×10^{-6}	1.2×10^{-4}	8.4×10^{-5}	2.0×10^{-5}	7.1×10^{-5}	3.1×10^{-4}	2.2×10^{-4}
F	-31.1	-42.7	-72.9	-30.3	-58.0	-78.2	-91.4	-79.3

Fig. 11. Scheme of the laser system optimized for the apodization exponent $N_d = 10$

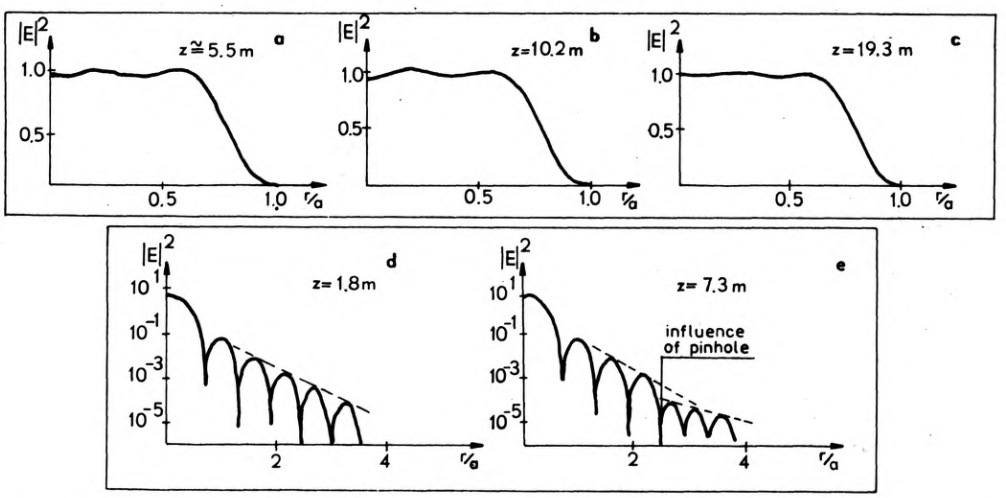

Fig. 12. Power density distributions in the planes of the rods: **a** — I, **b** — V, **c** — VIII in the optimized laser system for $N_d = 10$ and in the focal planes of the first spatial filter — **d** and the second filter — **e**. The influence of the pinhole located in the first filter is visible

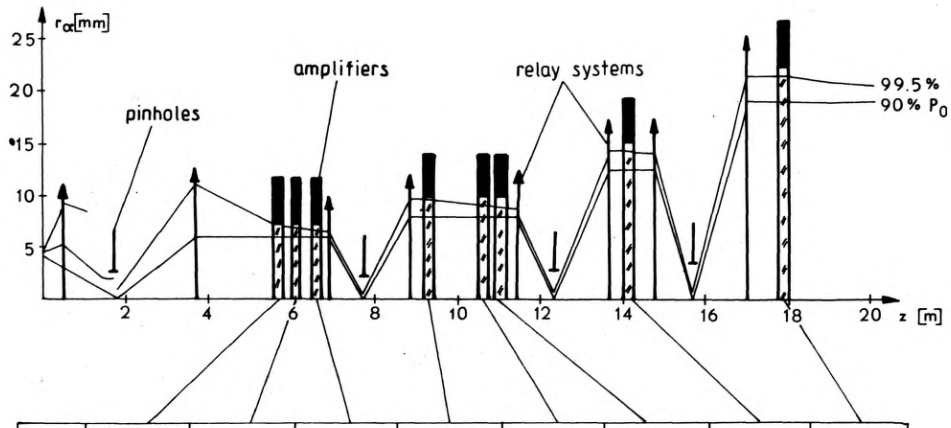

W_w	0.763	0.759	0.759	0.760	0.758	0.758	0.789	0.821
ϱ_c	2.48×10^{-2}	1.74×10^{-3}	1.12×10^{-3}	1.12×10^{-2}	1.94×10^{-3}	2.42×10^{-4}	6.77×10^{-3}	1.45×10^{-2}
$\Delta P/P_0$	4.45×10^{-3}	1.70×10^{-4}	1.04×10^{-4}	1.45×10^{-3}	2.17×10^{-4}	2.06×10^{-5}	5.41×10^{-4}	9.47×10^{-4}
F	-24.6	-32.0	-50.2	-25.7	-45.6	-59.8	-36.4	-33.8

Fig. 13. Scheme of the partly optimized laser. The initial distribution of the power density in the beam has been assumed to be close to rectangular for $N_0 = 100$

distribution in cross-section close to the rectangular one has been assumed, namely, $E_0(r) = \exp[-3.455(r/a)^{100}]$. The assumption of such an initial field distribution was due to the necessity of raising the global fill factor in the channel (increment of the effectiveness of energy extraction from the amplifiers) on the one hand, and to the needed analysis of the filtration influence on the spatial distribution in the propagating beam of high apodization exponent, on the other. It should be mentioned that the actual trends towards the application of the field distributions of relatively high apodization exponent to the high power laser channels follows from the necessity of diminishing the influence of the so-called global self-focusing on the space-time paramerters of the laser pulse, as well.

In Figure 14 the influence of filtration on the distributions in the output planes of the selected rods (I, V, VIII) has been illustrated for the beam on the input of the system with the apodization exponent $N_d = 100$. The filtration has been performed in such a way that the diaphragms (pinholes) of the diameter equal to the external diameter of the third Airy ring were placed in the focal planes of the filters. As it follows from Fig. 14 the introduction of the pinholes resulted in significant smoothing of the distributions in the planes of particular heads.

When comparing the modulation frequencies of the solution from Fig. 13 with these in Figs. 3 and 4 it should be stated that the influence of the filtration is unquestionable, the quantitative description for the applied values R_{max}, Δr, N_0 and $N_d = 100$ is however charged with some error. In accordance with the discussion carried out in Sect. 3 the results obtained for $N_d = 10$ are fully reliable.

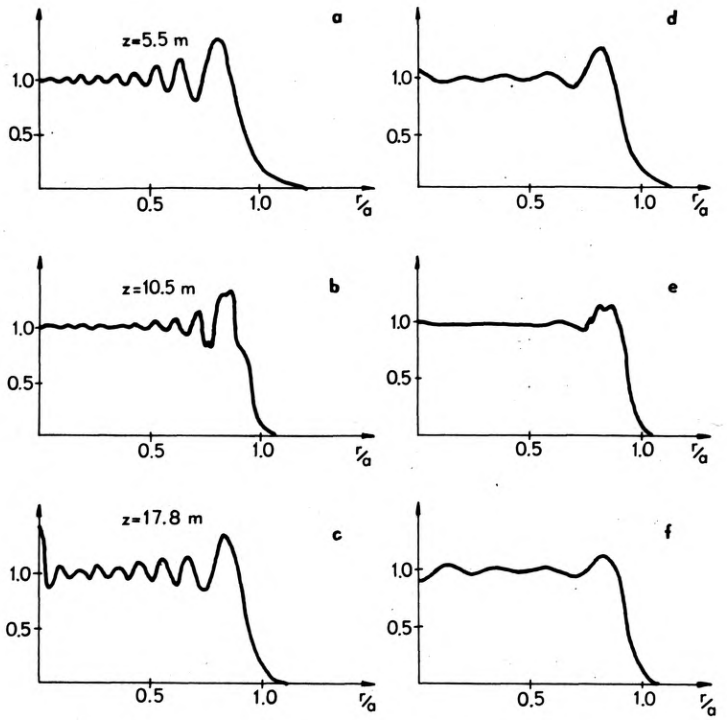

Fig. 14. Influence of filtration on the power density distribution on the fronts of the rods: **a**, **d** — I, **b**, **e** — V, **c**, **f** — VIII (**a**, **b**, **c** — distributions without filtration, **d**, **e**, **f** — distributions with filtration). Scheme of the laser system in Fig. 13

So far, the perturbations of the wavefront of the beam have not been taken into account. In the laser system containing the pinhole all the perturbations of the beam wavefront result in a shift of focal planes and in changes in the spatial field distributions. The pinholes are usually located in the focal plane where the beam diameter is the smallest. The spatial filters adjusted to the nonperturbed beam may significantly reduce the transmission in the case of the phase-perturbed beam. The deformations of the wavefront may occur due to both thermooptic effects in the active medium and self-focusing. For the assumed power density levels the self-focusing plays a small part in the lasers under test. In practice, the laser operation is essentially influenced by the thermooptic effects. We are going to consider this phenomenon [11]–[14].

The pumping of the active medium is inevitably associated with the heating effects. The inversion of population and an increase in temperature increment are usual nonuniform in the rod cross-section, while, as it is well known, the refractive index of the optical materials depends on their temperature. The temperature increment in the rod amounts usually to several (but less than 10) degrees [11]–[14].

For small range of temperature changes the relation is linear

$$\Delta n = \beta \Delta T \tag{16}$$

where: Δn – increment of the refractive index, ΔT – temperature increment. The coefficient β depends on the sort of the optical material and reaches the value of 10^{-6}–10^{-5} (it may be also negative).

In accordance with the model described in [11] we assume that the temperature increment (and that of the refractive index) of the active material may be expressed by the approximation formula

$$\Delta T(r) \simeq T_0 + a_1 r^2 + a_2 r^4 + a_3 r^6 + \ldots \tag{17}$$

where: r – current radius, a_i – constants dependent on the head construction, sort of active material, power of the pumping, etc.

The nonuniform heating of the rod causes:

– volume change of the refractive index,

– change in frontal surface shape of the rods due to nonuniform dilatation,

– induced birefringence connected with the thermal stress.

We are not intending to treat more deeply the thermooptic effects. Therefore, we shall neglect the induced birefringence (its encounting for cylindric symmetry is impossible) as well as the deformations of the front surfaces. We assume that the refractive index in the active material during the passage of the pulse is established and depends on the coordinate (r) according to the formula

$$n(r) = n_0 + n_1 (r/b)^2 + n_2 (r/b)^4 \tag{18}$$

where b – rod radius. The simplified model suffices to describe qualitatively both the motion of the beam focal plane and the drop of spatial filter transmission caused by this effect.

In the system, the scheme of which is shown in Fig. 11, radially changing refractive index of the rods has been given additionally

$$n(r) = n_0 - 3 \times 10^{-6} (r/b); \quad b = 7.5 \text{ mm} \tag{19}$$

(rods I, II, III). The value of the numerical coefficient 3×10^{-6} results from the energy balance. Namely, it has been assumed that 2% of energy collected in the battery of condensors is transformed to heat emerging in the rod volume. Under this assumption and taking account of both the material data for the glass GLS 1 (specific heat, thermooptic coefficient) and energy balance the mentioned coefficient value in formula (19) may be evaluated to be equal to 3×10^6. This way of estimating the thermooptic effects has been assumed also in the cases discussed below. In accordance with the estimation given in [13], the rods of such distribution of the refractive index focus the beam propagating inside these rods. As it has been shown by the respective calculations the focal plane of the beam in the second filter was shifted as a result of additional focusing on the laser rods of ⌀ 15 mm from the position 7440 mm to 7384 mm (i.e., about 56 mm), while the transmission of the pinhole dropped from 99.97% to 94.3%. From the point of view of the energy balance this loss of power is rather small, it however, changed in a definite way the density distributions in the sequent heads of ⌀ 20 (IV, V and VI). For example, the power distribution in the front plane of the V rod is shown in Fig. 15. When

comparing Figs. 15**a** and 12**b** we see that due to displacement of the focal plane of the beam and to the changed filtering conditions the uniform distribution (Fig. 12**b**) has been strongly deformed (Fig. 15**a**).

In the sequent heads ⌀ 20 (IV, V, VI) the refractive index was changed accordingly to fulfil the relation

$$n(r) = n_0 - 1.6 \times 10^{-6}(r/b)^2; \quad b = 10 \text{ mm}. \tag{20}$$

The numerical coefficient was estimated by using the energy balance method described above.

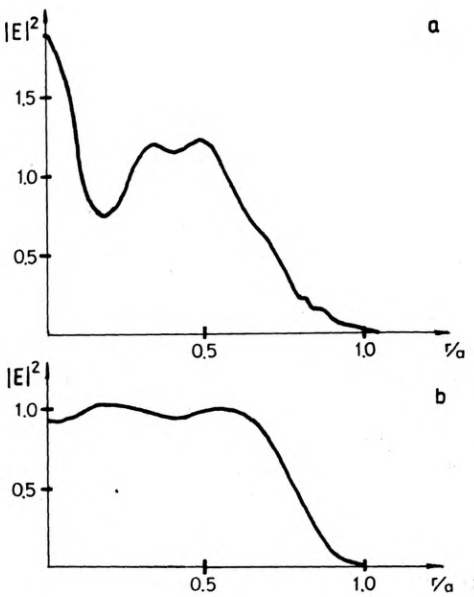

Fig. 15. Influence of the thermooptical focusing and connected with it shift of the focal plane of the beam with respect to the pinhole on the power density distribution in the input plane of the rod V: **a** — with pinhole, **b** — without pinhole

Due to the sequent additional focusing on the rods ⌀ 20 (IV, V, VI) the relaying of the third filters dropped to the value 58%, while the shift (toward the origin of the system) of the focal plane amounted to about 47 mm. As we have seen, a too strong action of the pinhole on the beam resulted in an essential deformation of the power density distribution. The distributions become again uniform when the diameter of the pinholes is increased without changing their positions (Fig. 15**b**). Therefrom it follows that in the laser system with filters the whole system must be adjusted so that focal plane of the beams during generation (while the rods heated during the pumping may focus or defocus additionally) be identical with the pinhole planes. Then neither any dramatic drop in the transmittance filter nor any worsening of the beam uniformity will occur.

The effect of focus displacement of the beam has been illustrated in Fig. 16. The lines plotted in this figure determine the region containing 50% and 90% of the total beam power. These lines have been obtained by integrating the power density of the

beam from $r = 0$ to such r_α, that

$$\alpha = \int_0^{r_\alpha} r|E|^2 dr \Big/ \int_0^{\infty} r|E|^2 dr \tag{21}$$

where α – given value (for instance, $\alpha = 0.5$ for 50%). The integration in (21) was performed usually once in the ten steps Δz.

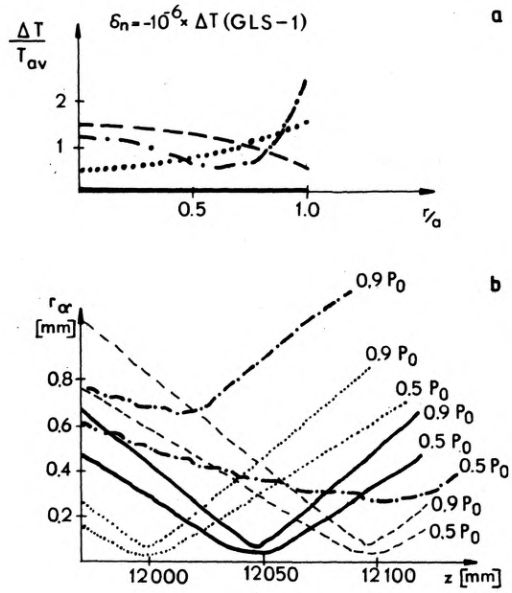

Fig. 16. Influence of the temperature distribution in rods on the course of the lines corresponding to the given per cent of the beam power: **a** – temperature distribution, **b** – line plot

If the refractive index in the rods changes according to the formula $n(r) = n_0 + n_1(r/b)^2$ then a shift of the beam focus along the z axis in the positive or negative direction depends on the sign of n_1 without changing the transversal sizes of the focus (no lens aberration accounted). By choosing the suitable constant n_1 the received shift may be such a one as that observed in the experimental system.

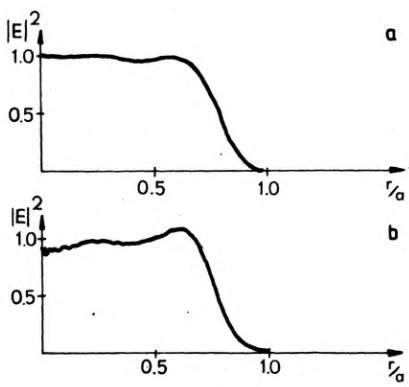

Fig. 17. Influence of the refractive index distribution in rods on the power density distribution in the rod output: **a** – $n(r) = n_0 + n_1(r/b)^2$, **b** – $n(r) = n_0 + n_1(r/b)^2 + n_2(r/b)^4$, $n_2 \neq 0$

If the refractive index changes according to the formula (18), where n_1 and n_2 are non-zero values, the beam at the rod output will be aberrated. This causes a significant widening of the transversal sizes of the focus (Fig. 16**b** – broken line), and the deformation of the power density distribution in the front planes of the rods (Fig. 17). Hence it is concluded that the way of changing the refractive index inside the rod is also of a great importance. An appropriate structure of the head may assure a parabolic change of the refractive index and then there occurs only a local shift which may be measured and taken into account in the design of the optical system of the laser channel.

The conclusions following from this work have been exploited to design a laser optical system in which the thermooptic beam defocusing by the rods (measured experimentally) was accounted [15].

5. Final remarks

In spite of some simplifications assumed in the model of the laser channel this work allowed us to explain some problems specific for the laser containing the relay systems and helped to better understand the principles of relaying and filtration.

In further works, we intend to present in the model of the laser system the influence of the phenomena, such as amplification and self-focusing, on the nonstationary time-space evaluation of the pulse.

Acknowledgements – We want to express our thanks to our friends Bogusław Kaczmarczyk, M. Sc., and Zbigniew Patron, M. Sc., for discussion which had some influence on the final form of this work.

References

[1] SIMMONS W. W., HUNT J. T., WARREN W. E., IEEE J. Quantum Electron. QE–**17** (1981), 1727.
[2] DUBIK A., FIRAK J., JACH K., Report of the Institute of Plasma Physics and Laser Microfusion, No. 4/80 (24), in Polish.
[3] FLECK J. A., MORRIS J. R., BLISS E. S., IEEE J. Quantum Electron. QE–**14**, (1978), 353.
[4] DUBIK A., JACH K., OWSIK J., Report of the Institute of Plasma Physics and Laser Microfusion, No. 9/80 (29), in Polish.
[5] DUBIK A., SARZYŃSKI A., J. Tech. Phys. **25** (1984), 441.
[6] SARZYŃSKI A., Report of the Institute of Plasma Physics and Laser Microfusion, No. 39/80 (59), in Polish.
[7] DUBIK A., SZCZUREK M., J. Tech. Phys. **25** (1984), 265.
[8] SIEGMAN A. E., Opt. Lett. **1** (1977), 13.
[9] SIEGMAN A. E., SZIKLAS E. A., Appl. Opt. **13** (1974), 2775.
[10] ARFKEN G., *Matematicheskie metody v fizike* (in Russian), Atomizdat (Ed.), Moskva 1970, p. 576.
[11] BELOSTOTSKII B. R., RUBANOV A. S. *Teplovoi rezhim tverdotelnovykh opticheskich generatorov* (in Russian), Energiya (Ed.), Moskva 1973.
[12] MARCZAK J. A., Master Thesis, Military Technical Academy, Warszawa 1973, in Polish (unpublished).
[13] TARASOV L. V., *Fizika protsessov v generatorakh kogerentnogo opticheskogo izlucheniya* (in Russian), Radio i Svyaz (Ed.), Moskva 1981.

[14] KERTES I., KONONKOV E. A., KRYUKOV P., SENATSKII I. V., CHEKALIN S. V., Zh. Ehksp. Teor. Phys. **59** (1970), 1115.
[15] KUŚNIERZ M., SZCZUREK M., Report of the Institute of Plasma Physics and Laser Microfusion, in preparation.

Received January 16, 1987

Дифракционная модель лазерного тракта в стационарном приближении

В работе описаны уравнения упрощенной модели лазерного тракта с пространственными фильтрами. Уравнения проблемы решались методом конечных разностей. Проведён анализ точности полученных численных решений. Приведены примеры оптимизации лазерного тракта для принятых критериев оптимальной установки. В модели учитывались: анодизация, ретрансляция и фильтрация излучения. Рассмотрены также следствия, которые могут возникать по поводу термооптической фокусировки (или же дефокусировки) лазерного пучка стержнями нагретыми во время накачки.